High-resolution cavity ringdown spectroscopy of the jet-cooled ethyl peroxy radical $C_2H_5O_2$

Gabriel M. P. Just,[1] Patrick Rupper,[1] Terry A. Miller,[1,a)] and W. Leo Meerts[2]
[1]*Department of Chemistry, Laser Spectroscopy Facility, The Ohio State University, 120 W. 18th Avenue, Columbus Ohio 43210, USA*
[2]*Molecular and Biophysics Group, Institute for Molecules and Materials, Radboud University, Nijmegen P.O. Box 9010, NL-6500 GL Nijmegen, The Netherlands*

(Received 14 September 2009; accepted 21 October 2009; published online 11 November 2009)

We have recorded high resolution, partially rotationally resolved, jet-cooled cavity ringdown spectra of the origin band of the $\tilde{A}-\tilde{X}$ electronic transition of both the G and T conformers of the perproteo and perdeutero isotopologues of the ethyl peroxy radical, $C_2H_5O_2$. This transition, located in the near infrared, was studied using a narrow band laser source ($\lesssim$250 MHz) and a supersonic slit-jet expansion coupled with an electric discharge allowing us to obtain rotational temperatures of about 15 K. All four spectra have been successfully simulated using an evolutionary algorithm approach with a Hamiltonian including rotational and spin-rotational terms. Excellent agreement with the experimental spectra was obtained by fitting seven molecular parameters in each ground and the first excited electronic states as well as the band origin of the electronic transition. This analysis unambiguously confirms the assignment of the lower frequency origin band to the G conformer and the higher frequency one to the T conformer. © *2009 American Institute of Physics*.
[doi:10.1063/1.3262612]

I. INTRODUCTION

Peroxy radicals ($RO_2\cdot$) play a crucial role in atmospheric chemistry and in low temperature combustion, which has been discussed in several overview articles.[1–4] A fundamental key to the understanding of the chemistry of gas phase reactions involving such reactive species is the ability to monitor the presence and concentrations of reactive intermediates in these reactions.[5–7] Due to the stringent demands for sensitivity and selectivity, the techniques of choice are usually spectroscopic[8] for whose application a prerequisite is well understood spectra.

Although the peroxy radicals possess a very strong $\tilde{B}-\tilde{X}$ electronic transition in the UV, centered near 240 nm, which has been routinely used in kinetic studies,[9] this transition is not suitable for high-resolution studies due to the repulsive nature of the $\tilde{B}$ state[10] resulting in a broad, structureless spectrum.[11] No species specificity, due to a lack of selectivity of the frequency of this transition to the R group in the peroxy radical, and no chance of resolving vibrational, rotational, and fine structure have shifted the high-resolution spectroscopic interest to the intrinsically sharp and well structured $\tilde{A}-\tilde{X}$ transition in the near-infrared (NIR), which was first observed by Hunziker and Wendt[12] several years ago, but is much weaker than the $\tilde{B}-\tilde{X}$ transition.

In the last couple of years, our group has investigated open-chain alkyl peroxy radicals with cavity ringdown spectroscopy (CRDS) ranging from methyl peroxy ($R=CH_3$) to pentyl peroxy ($R=C_5H_{11}$) [13–19] under ambient temperature conditions in a cell. We demonstrated the suitability of the NIR transition as a species specific, as well as an isomer and even conformer specific, diagnostic technique.[20] However, congestion due to the population of many rotational levels as well as overlap of conformers at room temperature prevents the extraction of spectroscopic parameters, such as rotational and spin-rotational constants, which are highly useful for benchmarking calculations. Other groups have used low to moderate resolution laser sources to study gas-phase methyl and ethyl peroxy by a variety of techniques, including negative-ion photoelectron spectroscopy,[21] photoionization,[22] cw-CRDS in the NIR,[23] and NIR absorption detected by time-of-flight mass spectroscopy,[24] but have similarly failed to obtain, with high precision, molecular parameters, characterizing the rotational and spin-rotational structure.

We recently developed an experimental apparatus combining a high-resolution laser source[25] with a jet-cooled CRDS setup[26] and have applied[27] this apparatus to record the rotationally resolved $\tilde{A}-\tilde{X}$ spectrum near 1.35 μm of the perdeuterated methyl peroxy radical, CD_3O_2. The experimental spectrum has been modeled using a Hamiltonian that includes the rigid body rotation of an asymmetric top and the spin-rotation interaction. An excellent quality least-squares fit was obtained to the model resulting in the high precision determination of 15 molecular parameters characterizing the $\tilde{A}$ and $\tilde{X}$ states.

Our recent CRDS studies of $C_2H_5O_2$ and $C_2D_5O_2$, under room-temperature conditions[17] identified the G and the T conformers of the radicals. However, due to the rotational congestion of these spectra, no accurate values of the rotational constants nor the spin-rotation constants were reported. This paper extends our previous work on CD_3O_2 to

a)Author to whom correspondence should be addressed. FAX: (614)292-1948. Electronic address: tamiller@chemistry.ohio-state.edu.

obtain and analyze the $\tilde{A}-\tilde{X}$ spectra for the ethyl peroxy radical under jet-cooled conditions with a narrowband laser source. We have found it of use to analyze and fit these spectra using an evolutionary algorithm approach thereby obtaining a set of high precision molecular parameters characterizing the $\tilde{A}$ and $\tilde{X}$ states of both ethyl peroxy conformers.

II. EXPERIMENTAL

A description of our high-resolution CRDS experimental setup has been given in detail in Refs. 25 and 28, so we will briefly summarize only the aspects particularly relevant to this work. The NIR radiation around 1.35 μm is obtained from the first Stokes of the stimulated Raman scattering (SRS) created by focusing the output of a pulsed, nearly Fourier-transform-limited (15 ns pulses), tunable, high energy ($\leq$100 mJ/pulse) Ti:Sapphire (Ti:Sa) laser source[25] into a stainless steel (1 m long) cell pressurized with typically 13 atm of H_2. The spectral broadening of the SRS radiation due to pressure and power broadening is estimated to be ~200 MHz (FWHM), resulting, when combined with the Doppler broadening from the slit-jet expansion, in an instrumental linewidth of ~250 MHz in the 1.3–1.4 μm range. The pulsed NIR radiation (~1 mJ) is coupled into the CRDS cavity, which consists of two high reflectivity mirrors (reflectivity > 99.995%) mounted on the arms of an evacuated chamber (0.67 m long). The mirrors are purged by a flow of inert gas argon to prevent a deposit from the reactive species onto the mirror surface.

The ethyl peroxy radicals $C_2H_5O_2$ are produced by expanding a mixture of ~1% ethyl iodide (C_2H_5I) and ~10% oxygen (O_2) in first run neon (75% Ne, 25% He) through a slit-jet (1 mm × 5 cm) nozzle (opening time 1 ms) and discharge (9 mm plasma channel length, 1 mm spacing between the electrodes). A high voltage is applied to the two stainless steel electrodes for ~200 μs during the gas pulse, resulting in plasma currents of ~300–400 mA. The precursor gas mixture is prepared by bubbling ~500 Torr of a O_2 and Ne gas mixture through a sample bomb containing C_2H_5I at –45 °C.

The SRS radiation beam probes the cooled supersonic gas expansion 10 mm downstream from the throat of the expansion, where the radical concentration is estimated to be $\sim 5\times 10^{12}$ molecules/cm^3.[27] An InGaAs detector measures the beam exiting the chamber. Ringdown times of up to 300 μs (corresponding to an absorption equivalent length of ~6 km) and an experimental sensitivity of 0.02 ppm/pass (corresponding to a noise equivalent absorption of 4.5 ppb Hz$^{-1/2}$) have been achieved using our best mirror set (Advanced Thin Films).

The spectra were recorded using frequency scans of ~10 GHz segments with a frequency step size of 50 MHz with 4 laser shots averaged at each frequency point. Each segment is linearized using a simultaneously recorded Fabry–Perot etalon trace (FSR ≈ 1 GHz). Calibration of the absolute frequency is achieved by using absorption from residual water in our CRDS spectrometer and matching the observed frequencies with those provided in the HITRAN database.[28]

III. THEORY

All the recorded spectra of the ethyl peroxy radicals involve the 0_0^0 band of the $\tilde{A}-\tilde{X}$ electronic transition. Since the radical is in a doublet state we expect both rotational structure and an observable spin-rotation interaction as has been seen with the alkoxy radicals.[8] Hence, the structure of each vibronic level should be described by the Hamiltonian,

$$\mathcal{H}_T = \mathcal{H}_{\mathrm{Rot}} + \mathcal{H}_{\mathrm{SR}} + T_0(i), \tag{1}$$

where $T_0(i)$ is the energy of the vibronic state (vibrationless level of $\tilde{A}$ or $\tilde{X}$ electronic state) with $i=\tilde{A}$ or $\tilde{X}$ and $T_0(\tilde{X})$ is taken as zero. We expect any hyperfine splittings to be well below our experimental resolution and neglect them in $\mathcal{H}_T$.

Due to the fact that the spin-rotation coupling is expected to be fairly small, we use a case (b) like basis, with the prolate symmetric top representation, $|JNKSM_J\rangle$ in which the rotational angular momentum, N, and the spin-angular momentum, S, are coupled to generate the resultant total angular momentum J. The M_J quantum number represents the projection of J on the space fixed Z axis and K denotes the projection of N on the a principal axis. We can now simply write the rotational Hamiltonian, $\mathcal{H}_{\mathrm{Rot}}$, in the principal axis system,

$$\mathcal{H}_{\mathrm{Rot}} = AN_a^2 + BN_b^2 + CN_c^2, \tag{2}$$

where A, B, and C denote, by convention, the rotational constants of the radical. The matrix elements of the rotational Hamiltonian, $\mathcal{H}_{\mathrm{Rot}}$, are well-known.[29,30]

The spin-rotation Hamiltonian has been examined by many authors[29,31–35] and can be written as

$$\mathcal{H}_{\mathrm{SR}} = \frac{1}{2}\sum_{\alpha,\beta} \epsilon_{\alpha\beta}(N_\alpha S_\beta + S_\beta N_\alpha), \tag{3}$$

where $\epsilon_{\alpha\beta}$ represent the different components of the spin-rotation tensor expressed in the same principal axis system.

It is well known that the components of the spin rotation tensor, $\epsilon_{\alpha\beta}$, have two contributions,[31,36,37] which can be expressed as

$$\epsilon_{\alpha\beta} = \epsilon_{\alpha\beta}^{(1)} + \epsilon_{\alpha\beta}^{(2)}, \tag{4}$$

where $\epsilon_{\alpha\beta}^{(1)}$ is defined as the first-order contribution resulting from the direct coupling between the electron spin and the magnetic field arising from the rotation of the molecule. Typically, this first order contribution to the spin-rotation tensor component is considered to be negligible with respect to the second order contribution, $\epsilon_{\alpha\beta}^{(2)}$, which arises from the interaction of the spin-orbit coupling and the Coriolis interaction. One can write the second order contribution to the tensor components, $\epsilon_{\alpha\beta}^{(2)}$, as

$$\epsilon_{\alpha\beta} \approx \epsilon_{\alpha\beta}^{(2)} = -2\sum_{j\neq i} \frac{\langle i|\hat{\xi}\hat{L}_\alpha|j\rangle\langle j|X_\beta L_\beta|i\rangle + c.c.}{E_i - E_j}. \tag{5}$$

In the above expression for $\epsilon^{(2)}_{\alpha\beta}$, ξ represents the spin-orbit coupling operator; L describes the electronic orbital angular momentum, and X_β represents the rotational constant for the β principal axis. Finally, i denotes the state of interest and the sum extends over all states j.

In principle the spin-rotation tensor contains nine parameters (three diagonal and six off-diagonal). On the other hand, Brown and Sears[36] have shown that, in the most general case, i.e., C_1 symmetry, which is appropriate for the G $C_2H_5O_2$ conformer, that only six out of the nine parameters are independently determinable from an experimental spectrum. For a molecule with C_s symmetry like T $C_2H_5O_2$, only four spin-rotation parameters are determinable. In the general case of a molecule with C_1 symmetry, a convenient way to express the tensor components is via their irreducible tensor combinations,

$$T^0_0(\tilde{\epsilon}) = \frac{-1}{\sqrt{3}}(\tilde{\epsilon}_{aa} + \tilde{\epsilon}_{bb} + \tilde{\epsilon}_{cc}) = \sqrt{3}a_0, \tag{6}$$

$$T^2_0(\tilde{\epsilon}) = \frac{1}{\sqrt{6}}(2\tilde{\epsilon}_{aa} - \tilde{\epsilon}_{bb} - \tilde{\epsilon}_{cc}) = -\sqrt{6}a, \tag{7}$$

$$T^2_{\pm 1}(\tilde{\epsilon}) = \mp \tfrac{1}{2}[(\tilde{\epsilon}_{ba} + \tilde{\epsilon}_{ab}) \pm i(\tilde{\epsilon}_{ca} + \tilde{\epsilon}_{ac})] = \pm (d \pm ie), \tag{8}$$

$$T^2_{\pm 2}(\tilde{\epsilon}) = \tfrac{1}{2}[(\tilde{\epsilon}_{bb} - \tilde{\epsilon}_{cc}) \pm i(\tilde{\epsilon}_{bc} + \tilde{\epsilon}_{cb})] = b \pm ic, \tag{9}$$

where the $\tilde{\epsilon}_{\alpha\beta}$ are the reduced tensor components of Brown and Sears[36] and where the spin rotation parameters, a_0, a, b, c, d, and e, were introduced by Raynes[32] and are used in our numerical analysis. While in principle (but not in practice–see below) all six Raynes parameters are necessary for the G conformer, c and e vanish by symmetry for the T conformer.

IV. SPECTRAL ANALYSIS AND SIMULATION

Historically, our group has used the approach of a least square fitting (LSF) procedure, employing the SPECVIEW software package,[38] in order to obtain molecular parameters from a high resolution spectrum. This approach is traditional and completely appropriate if one has a well resolved spectrum for which individual line assignments are possible.

However the applicability of such an approach is limited when one has only partially resolved spectra such as are shown in Fig. 1 for the G conformers of $C_2H_5O_2$ and $C_2D_5O_2$. Under these conditions, unique transition assignments are nearly impossible as most features in the spectra correspond to multiple (~2–5) overlapping transitions. In order to fit such complicated spectrum, we decided to use the evolutionary algorithm[39] (EA), which has been proven to provide reliable results for semiautomated fits of both fully and partially resolved spectra.[39–42]

A. Fitting with an evolutionary algorithm approach

The EA is a method based on a Darwinian approach. In nature, natural selection occurs by reproduction with mutation of genes leading to only the best adapted individuals surviving. From a spectroscopic point of view, the EA approach reproduces this behavior to fit an experimental spectrum with a model based upon the differences of the eigenvalues of the Hamiltonian such as $\mathcal{H}_T$ given by Eq. (1). Each of the molecular parameters in $\mathcal{H}_T$ can be thought of as a gene. For the ethyl peroxy $\tilde{A}-\tilde{X}$ spectra the parameters of the model are mutated like genes, to select a set, corresponding to the chromosome, which ultimately best reproduces the experimental spectra. The evolution to the "best fit" chromosome is determined by how well a spectral simulation, based on a given chromosome, resembles the experimental result. In this work, a chromosome is formed from 18 genes corresponding to the parameters that are fitted. These include the 15 total molecular parameters of $\mathcal{H}_T$, i.e., three rotational and four spin-rotational constants for each the ground and first excited electronic state and the band origin (T_{00}), as well as the rotational temperature, and the two angles θ and ϕ describing the orientation of the electric dipole moment with respect to the principal axis system. During the initial step of the fit, values for all the parameters, i.e., genes, are randomly set between the upper and lower limits input by the user. (See below the process for choosing these limits.) Typically a total of 567 chromosomes are generated.

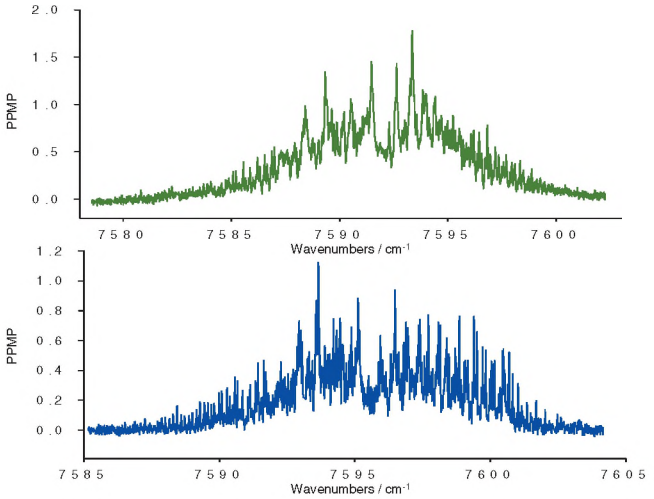

FIG. 1. The top green trace is the high resolution jet-cooled experimental CRDS spectrum of the G conformer of the $C_2H_5O_2$ radical. The bottom blue trace represents the high resolution jet-cooled experimental CRDS spectrum of the G conformer of the $C_2D_5O_2$ radical. The vertical axis gives the absolute absorption in parts per million per pass (ppmp) as a function of laser frequency along the horizontal axis.

The next generation of chromosomes is generated from the selected best parent(s) (highest fitness) using an evolution strategy with mutative step size control. Mutative step size control adapts the speed at which the parameter space is explored with each optimization step. It tends to work well for the adaptation of a global step size but tends to fail when it comes to the step size of each individual parameter due to several disruptive effects.[43] The derandomized algorithm DR2 used here[44] is aiming at the accumulation of information about the correlation or anticorrelation of past mutation vectors that connect trial solutions in order to tackle this problem. The high effectiveness of this approach for spectral analysis has been demonstrated recently.[45,46]

As mentioned previously, the quality of the match be-

tween the experimental spectrum and a given simulation is evaluated by a fitness function, F_{fg}. It has been shown by Hageman[41] that F_{fg} can be defined as

$$F_{fg} = \frac{\sum_{r=-l}^{l} w(r) \sum_{i=1}^{N} f(i)g(i+r)}{\sqrt{\sum_{r=-l}^{l} w(r) \sum_{i=1}^{N} f(i)f(i+r)} \sqrt{\sum_{r=-l}^{l} w(r) \sum_{i=1}^{N} g(i)g(i+r)}}. \tag{10}$$

In the above f represents the experimental spectrum while g represents the simulated spectrum. The function $w(r)$ is called the overlap function and controls the sensitivity of the fitness function for a shift of the experimental and simulated spectra relative to each other.

If both the experimental and simulated spectra are viewed as vectors with N dimensions (frequency points), then the numerator of F_{fg} is a weighted dot product of these vectors and the denominator is simply a normalization factor, i.e.,

$$F_{fg} = \frac{(\boldsymbol{f},\boldsymbol{g})}{\|\boldsymbol{f}\|\|\boldsymbol{g}\|}, \tag{11}$$

where the dot product $(\boldsymbol{f},\boldsymbol{g})$ includes the weighting function $\omega(r)$ and the norms of $\boldsymbol{f}$ and $\boldsymbol{g}$ are defined as

$$\|\boldsymbol{f}\| = \sqrt{(\boldsymbol{f},\boldsymbol{f})} \tag{12}$$

and

$$\|\boldsymbol{g}\| = \sqrt{(\boldsymbol{g},\boldsymbol{g})}. \tag{13}$$

It has been found[41] that $w(r)$ can be equated to a simple triangular function with a basewidth of 2ℓ points,

$$w(r) = \begin{cases} 1 - |r|/\ell & \text{for} |r| < \ell \\ 0 & \text{otherwise} \end{cases}, \tag{14}$$

with ℓ typically being chosen as the half-width at half-height of a fully resolved transition.

The EA is very suitable for parallel computation. The calculations were performed on a Linux cluster in Nijmegen based on SUN Fire X4100 and X4150 machines. Typically 32 CPUs were used. Convergence occurs in approximately 200 generations corresponding to a wall clock time of about 20 min.

In order to achieve fast convergence, a wise choice for the initial ranges of the different parameters in $\mathcal{H}_T$ is needed. Initially, we chose the predicted rotational constants from a B3LYP calculation and assumed a search range of $\pm 2\%$. After observing that the fitted results were in significantly better agreement with the values from the full second order Møller-Plesset [MP2(FULL)] calculation (see discussion below) we used them with a range of $\pm 0.25\%$ as our starting point in the fits. For the spin-rotation constants we used the procedure described in Sec. V to estimate their values and assumed a search range of 10^{-1} to 10^{+1} times the predicted value.

V. ELECTRONIC STRUCTURE, CALCULATIONS, AND MOLECULAR PARAMETER ESTIMATION

In order for the EA approach to be effective, one needs to define *a priori* a range within which each parameter value may lie. Electronic structure calculations are very useful in setting these ranges. After the spectrum has been fit by the EA approach, the fit parameter values can in turn be used to benchmark the quality of particular electronic structure methods.

Using the GAUSSIAN 03 software package,[47] we computed the global minima for each the G and T conformers, both ground, $\tilde{X}$, and first excited, $\tilde{A}$, electronic states using different methods and basis sets. These included a density functional theory (DFT) method (B3LYP) with a 6-31 +g(d) basis set, which represents a fairly inexpensive calculation. We also used a MP2 (FULL) perturbation calculation with a 6–31g(d) basis set. The latter set of calculation has been chosen since it has been shown that, in the case of the alkyl peroxy radicals, the G2 composite method yields very accurate T_{00} values.[20] Hence, the optimized geometry from the G2 method, which is MP2(FULL)/6–31g(d),[48] ought to be fairly representative of the electronic eigenenergies and corresponding geometries of the molecule, which are necessary for calculations of, respectively, the T_{00} values and rotational constants. The final method used was the coupled cluster singlet and doublet, CCSD [6–31g(d)]. This is a somewhat more computationally expensive method and would be of considerable interest to benchmark. For the components of the dipole moments, we turned to a configuration interaction, singles, CIS, method with a 6-31g+(d) basis. We performed the calculation at the $\tilde{X}$ state geometries found by each the CCSD, B3LYP, and MP2 methods.

In order to predict the T_{00} electronic transition by the CCSD and B3LYP methods, we computed the vibrational frequencies for each method and made the zero point energy (ZPE) correction. The T_{00} value from the MP2 calculation is actually from the G2 method and hence it already contains extra correction terms including the ZPE. It also should be noted that all the corresponding rotational constants have been calculated for the equilibrium geometry and not for the experimentally observed vibrationless level. However since zero-point corrections for rotational constants are typically less than a few tenths of a percent, this only mildly affects comparison between the calculated and observed values. Tables I–IV summarize the rotational constants and T_{00} values calculated via the different electronic structure calculations.

There is no electronic structure package that directly calculates spin-rotational coupling constants so we use a semiempirical approach. Recently, our group simulated the high resolution, jet cooled CRDS spectrum of the CD_3O_2 radical. We experimentally determined[27] for CD_3O_2 the rotational constants in both the $\tilde{X}$ and the $\tilde{A}$ states and four components of the spin rotation tensor for this C_s symmetry molecule, i.e., ϵ_{aa}, ϵ_{bb}, ϵ_{cc}, and $\frac{1}{2}(\epsilon_{ab}+\epsilon_{ba})$. Brown, Sears and Watson showed that, in the inertial axis system, one could relate the reduced spin-rotation tensor component of two isotopologues via the following transformation:

TABLE I. Molecular parameters of G conformer of $C_2D_5O_2$ radical from the experimental spectrum and from the indicated electronic structure calculations (see text for details). The calculated T_{00} has been corrected by the scaled ZPE correction according to the NIST website (http://cccbdb.nist.gov/vibscalejust.asp) under the harmonic oscillator assumption. The numbers in square brackets represent the percent deviation of the predicted constant with respect to the fitted results with the corresponding experimental percentage uncertainty in parentheses. The calculated and predicted constants are for the equilibrium geometry. The components of the transition moment are computed using the CIS method using the optimized geometries indicated from the normalized dipole moment.

Const. (cm^{-1})	Fit[a]	MP2(FULL)\6–31g(d)	CCSD\6-31+g(d)	B3LYP\6-31+g(d)
A''	0.44963 (3)	0.45106 [−0.318 (7)]	0.4458 [1.123 (7)]	0.45608 [−1.435 (7)]
B''	0.16298 (2)	0.16387 [−0.55 (1)]	0.16211 [0.53 (1)]	0.15784 [3.15 (1)]
C''	0.14083 (2)	0.14182 [−0.70 (1)]	0.13995 [0.62 (1)]	0.13805 [1.97 (1)]
$\tilde{\epsilon}''_{aa}=-(a_0+2a)''$	−0.0115 (5)	−0.0114 (15) [0.9 (43)]	−0.0113 (15) [1.7 (43)]	−0.0122 (15) [−6.1 (43)]
$\tilde{\epsilon}''_{bb}=(a+b-a_0)''$	−0.0064 (4)	−0.0062 (14) [3. (6)]	−0.0062 (14) [3. (6)]	−0.0056 (14) [12. (6)]
$\tilde{\epsilon}''_{cc}=(a-b-a_0)''$	−0.0023 (5)	−0.0031 (15) [−34. (21)]	−0.0030 (15) [−30. (21)]	−0.0032 (15) [−39. (21)]
$(1/2)(\tilde{\epsilon}_{ab}+\tilde{\epsilon}_{ba})''=d''$	−0.0084 (11)	−0.0061 (22) [27. (13)]	−0.0060 (22) [28. (13)]	−0.0063 (22) [25. (13)]
$(1/2)(\tilde{\epsilon}_{bc}+\tilde{\epsilon}_{cb})''=c''$	⋯	0.0036 [⋯]	0.0035 [⋯]	0.0034 [⋯]
$(1/2)(\tilde{\epsilon}_{ac}+\tilde{\epsilon}_{ca})''=e''$	⋯	0.0011 [⋯]	0.0010 [⋯]	0.0014 [⋯]
A'	0.42660 (3)	0.42703 [−0.101 (7)]	0.42102 [1.308 (7)]	0.43081 [−0.987 (7)]
B'	0.16560 (2)	0.16638 [−0.47 (1)]	0.16542 [0.65 (1)]	0.16099 [2.78 (1)]
C'	0.14046 (2)	0.14134 [−0.63 (1)]	0.13934 [0.80 (1)]	0.13710 [2.39 (1)]
$\tilde{\epsilon}'_{aa}=-(a_0+2a)'$	0.0108 (5)	0.0135 (15) [−25. (5)]	0.0136 (15) [−26. (5)]	0.0147 (15) [−36. (5)]
$\tilde{\epsilon}'_{bb}=(a+b-a_0)'$	0.0080 (4)	0.0071 (14) [11. (5)]	0.0070 (14) [13. (5)]	0.0065 (14) [18. (5)]
$\tilde{\epsilon}'_{cc}=(a-b-a_0)'$	0.0006 (4)	0.0009 (15) [−50. (66)]	0.0008 (15) [−33. (66)]	0.0008 (15) [−33. (66)]
$(1/2)(\tilde{\epsilon}_{ab}+\tilde{\epsilon}_{ba})'=d'$	0.0098 (6)	0.0100 (22) [−2. (6)]	0.0099 (22) [−1. (6)]	0.0101 (22) [−3. (6)]
$(1/2)(\tilde{\epsilon}_{bc}+\tilde{\epsilon}_{cb})'=c'$	⋯	−0.0035 [⋯]	−0.0034 [⋯]	−0.0033 [⋯]
$(1/2)(\tilde{\epsilon}_{ac}+\tilde{\epsilon}_{ca})'=e'$	⋯	−0.0006 [⋯]	−0.0006 [⋯]	−0.0007 [⋯]
T_{00}	7595.1855 (4)	7582.3000 [0.17]	7094.7782 [6.59]	7668.0560 [−0.96]
$\lvert\mu_a/\mu_b\rvert$ [b]	0.569	0.263	0.289	0.315
$\lvert\mu_c/\mu_b\rvert$ [b]	0.639	0.438	0.434	0.342

[a]Fit temperature of 14.8 K.
[b]Determined from fit values of $\theta=60.0°$, $\phi=60.7°$.

$$I_R\tilde{\epsilon}_R = I_S\tilde{\epsilon}_S, \tag{15}$$

where I represent the moment of inertia tensor and $\tilde{\epsilon}$ the reduced spin-rotation tensor in the respective principal axis systems, with R denoting the reference molecule and S the isotopologue of interest. Tarczay *et al.*[49] extended this procedure to relate the components of the spin-rotation tensor for any molecule in the same family. The basic physical requirement for the Tarczay extension is that the electronic transition be localized on a given chromophore with common electronic structure for all the family members. Under these circumstances, structural modifications to the rest of the molecule will reorient the principal inertial axes and change the values of tensor components expressed along them but leave unchanged the spin-rotational tensor components expressed in a local axis system tied to the chromophore. Radicals like methyl and ethyl peroxy seem likely to be well described by this physical picture since for all the open-chain primary alkoxy radicals the electronic transition is localized on the O_2 chromophore. A convenient local frame for the peroxy radicals has the z axis along the O_2 bond with x and y coinciding with the p orbitals perpendicular to it. We therefore conclude that in the local frame,

$$(I_S\tilde{\epsilon}_S)^{\mathrm{loc}} = (I_R\tilde{\epsilon}_R)^{\mathrm{loc}}. \tag{16}$$

If U is the unitary transformation relating the local and principal axes system then

$$U_S I_S \tilde{\epsilon}_S U_S^{-1} = U_R I_R \tilde{\epsilon}_R U_R^{-1} \tag{17}$$

or

$$\tilde{\epsilon}_S = I_S^{-1} U_S^{-1} U_R I_R \tilde{\epsilon}_R U_R^{-1} U_S, \tag{18}$$

where $\tilde{\epsilon}_S$ is expressed in the principal axis system. Both the I and the U matrices are solely dependent upon the geometry of the molecule and hence can be calculated from the optimized geometry of the electronic structure calculation. We use the spin-rotation tensor ϵ_R, experimentally determined for CD_3O_2, as the reference molecule to calculate ϵ_S for $C_2H_5O_2$.

VI. EXPERIMENTAL RESULTS

A. The G conformer of the ethyl peroxy radical

Ethyl peroxy is the simplest alkyl peroxy radical that has more than one conformer. As noted previously its conformers can be labeled as G (CCOO dihedral angle ±60°), which has a C_1 symmetry, and T (CCOO dihedral angle of ±180°), which has C_s symmetry. In 2007, Rupper *et al.*[17] observed and analyzed the room temperature CRDS spectra of both conformers of this radical. Based upon high level quantum chemistry calculations, they determined that the G conformer was about 80 cm^{-1} lower in energy than the T conformer in the $\tilde{X}$ state. Therefore, we decided to first investigate the G conformer 0_0^0 band with our high resolution jet-cooled appa-

TABLE II. Molecular parameters of G conformer of $C_2H_5O_2$ radical. The calculated T_{00} has been corrected by the scaled ZPE correction according to the NIST website (http://cccbdb.nist.gov/vibscalejust.asp) under the harmonic oscillator assumption. The numbers in square brackets represent the percent deviation of the predicted constant with respect to the fitted results with the corresponding experimental percentage uncertainty in parentheses. The calculated and predicted constants are for the equilibrium geometry. The components of the transition moment are computed using the CIS method using the optimized geometries indicated from the normalized dipole moment.

Const. (cm^{-1})	Fit[a]	MP2(FULL)\6–31g(d)	CCSD\6-31+g(d)	B3LYP\6-31+g(d)
A''	0.59099 (6)	0.59373 [−0.46 (1)]	0.58427 [1.14 (1)]	0.60182 [1.83 (1]
B''	0.18899 (3)	0.19055 [−0.83 (2)]	0.18845 [0.29 (2)]	0.18348 [−2.92 (2)]
C''	0.16299 (4)	0.16459 [−0.98 (2)]	0.16233 [0.40 (2)]	0.16018 [−1.72 (2)]
$\tilde{\epsilon}''_{aa}=-(a_0+2a)''$	−0.0168 (8)	−0.0150 (15) [11. (5)]	−0.0149 (15) [11. (5)]	−0.0160 (15) [−5. (5)]
$\tilde{\epsilon}''_{bb}=(a+b-a_0)''$	−0.0078 (6)	−0.0072 (14) [8. (8)]	−0.0072 (14) [8. (8)]	−0.0065 (14) [−17. (8)]
$\tilde{\epsilon}''_{cc}=(a-b-a_0)''$	−0.0010 (6)	−0.0036 (15) [−260. (60)]	−0.0035 (15) [−250. (60)]	−0.0036 (15) [260. (60)]
$(1/2)(\tilde{\epsilon}_{ab}+\tilde{\epsilon}_{ba})''=d''$	−0.0085 (8)	−0.0078 (22) [8. (9)]	−0.0077 (22) [9. (9)]	−0.0081 (22) [−5. (9)]
$(1/2)(\tilde{\epsilon}_{bc}+\tilde{\epsilon}_{cb})''=c''$	⋯	0.0042 [⋯]	0.0041 [⋯]	0.0040 [⋯]
$(1/2)(\tilde{\epsilon}_{ac}+\tilde{\epsilon}_{ca})''=e''$	⋯	0.0014 [⋯]	0.0013 [⋯]	0.0018 [⋯]
A'	0.55305 (5)	0.55366 [−0.110 (9)]	0.54517 [1.425 (9)]	0.56147 [1.522 (9)]
B'	0.19250 (5)	0.19398 [−0.77 (3)]	0.19172 [0.41 (3)]	0.18734 [−2.68 (3)]
C'	0.16239 (3)	0.16380 [−0.87 (2)]	0.16137 [0.63 (2)]	0.15878 [−2.22 (2)]
$\tilde{\epsilon}'_{aa}=-(a_0+2a)'$	0.0145 (8)	0.0175 (15) [−21. (6)]	0.0176 (15) [−21. (6)]	0.0192 (15) [32. (6)]
$\tilde{\epsilon}'_{bb}=(a+b-a_0)'$	0.0095 (5)	0.0083 (14) [13. (5)]	0.0081 (14) [15. (5)]	0.0076 (14) [−20. (5)]
$\tilde{\epsilon}'_{cc}=(a-b-a_0)'$	0.0011 (6)	0.0010 (15) [9. (55)]	0.0009 (15) [18. (55)]	0.0009 (15) [−18. (55)]
$(1/2)(\tilde{\epsilon}_{ab}+\tilde{\epsilon}_{ba})'=d'$	0.0115 (12)	0.0126 (22) [−10. (10)]	0.0125 (22) [−9. (10)]	0.0128 (22) [11. (10)]
$(1/2)(\tilde{\epsilon}_{bc}+\tilde{\epsilon}_{cb})'=c'$	⋯	−0.0040 [⋯]	−0.0039 [⋯]	−0.0038 [⋯]
$(1/2)(\tilde{\epsilon}_{ac}+\tilde{\epsilon}_{ca})'=e'$	⋯	−0.0008 [⋯]	−0.0007 [⋯]	−0.0009 [⋯]
T_{00}	7591.5831 (5)	7579.7980 [0.16]	7090.8280 [6.60]	7663.3756 [−0.95]
$\lvert\mu_a/\mu_b\rvert$[b]	0.678	0.263	0.289	0.315
$\lvert\mu_c/\mu_b\rvert$[b]	0.739	0.438	0.434	0.342

[a]Fit temperature of 16.2 K.
[b]Determined from fit values of $\theta=55.7°$, $\phi=58.8°$.

TABLE III. Molecular parameters of T conformer of $C_2H_5O_2$ radical. The calculated T_{00} has been corrected by the scaled ZPE correction according to the NIST website (http://cccbdb.nist.gov/vibscalejust.asp) under the harmonic oscillator assumption. The numbers in square brackets represent the percent deviation of the predicted constant with respect to the fitted results with the corresponding experimental percentage uncertainty in parentheses. The calculated and predicted constants are for the equilibrium geometry.

Const. (cm^{-1})	Fit[a]	MP2(FULL)\6–31g(d)	CCSD\6-31+g(d)	B3LYP\6-31+g(d)
A''	1.10180 (7)	1.10657 [−0.433 (6)]	1.10128 [0.047 (6)]	1.11307 [−1.023 (6)]
B''	0.14766 (6)	0.14890 [−0.84 (4)]	0.14680 [0.58 (4)]	0.14577 [1.28 (4)]
C''	0.13725 (6)	0.13810 [−0.62 (4)]	0.13627 [0.71 (4)]	0.13553 [1.25 (4)]
$\tilde{\epsilon}''_{aa}=-(a_0+2a)''$	−0.0751 (11)	−0.0691 (15) [8. (1)]	−0.0687 (15) [9. (1)]	−0.0692 (15) [8. (1)]
$\tilde{\epsilon}''_{bb}=(a+b-a_0)''$	−0.0027 (8)	−0.0032 (14) [−19. (30)]	−0.0032 (14) [−19. (30)]	−0.0032 (14) [−19. (30)]
$\tilde{\epsilon}''_{cc}=(a-b-a_0)''$	−0.0004 (8)	−0.0001 (15) [75. (200)]	−0.0001 (15) [75. (200)]	−0.0001 (15) [75. (200)]
$(1/2)(\tilde{\epsilon}_{ab}+\tilde{\epsilon}_{ba})''=d''$	0.0064 (23)	0.0042 (22) [34. (36)]	0.0043 (22) [33. (36)]	0.0047 (22) [27. (36)]
$(1/2)(\tilde{\epsilon}_{bc}+\tilde{\epsilon}_{cb})''=c''$	0	0	0	0
$(1/2)(\tilde{\epsilon}_{ac}+\tilde{\epsilon}_{ca})''=e''$	0	0	0	0
A'	1.06663 (7)	1.06776 [−0.106 (7)]	1.06278 [0.361 (7)]	1.08167 [−1.410 (7)]
B'	0.14844 (6)	0.14932 [−0.59 (4)]	0.14689 [1.04 (4)]	0.14581 [1.77 (4)]
C'	0.13715 (6)	0.13784 [−0.50 (4)]	0.13575 [1.02 (4)]	0.13510 [1.49 (4)]
$\tilde{\epsilon}'_{aa}=-(a_0+2a)'$	0.0790 (14)	0.0731 (15) [7. (2)]	0.0724 (15) [8. (2)]	0.0724 (15) [8. (2)]
$\tilde{\epsilon}'_{bb}=(a+b-a_0)'$	0.0042 (8)	0.0033 (14) [21. (19)]	0.0033 (14) [21. (19)]	0.0035 (14) [17. (19)]
$\tilde{\epsilon}'_{cc}=(a-b-a_0)'$	−0.0028 (8)	−0.0014 (15) [50. (29)]	−0.0014 (15) [50. (29)]	−0.0014 (15) [50. (29)]
$(1/2)(\tilde{\epsilon}_{ab}+\tilde{\epsilon}_{ba})'=d'$	−0.0215 (8)	−0.0125 (22) [42. (4)]	−0.0127 (22) [41. (4)]	−0.0136 (22) [37. (4)]
$(1/2)(\tilde{\epsilon}_{bc}+\tilde{\epsilon}_{cb})'=c'$	0	0	0	0
$(1/2)(\tilde{\epsilon}_{ac}+\tilde{\epsilon}_{ca})'=e'$	0	0	0	0
T_{00}	7361.8209 (10)	7355.5394 [0.09]	6921.0712 [5.99]	7508.3958 [1.99]

[a]Fit temperature of 99.3 K. By symmetry only the c component of the dipole moment is nonzero.

TABLE IV. Molecular parameters of T conformer of $C_2D_5O_2$ radical. The calculated T_{00} has been corrected by the scaled ZPE correction according to the NIST website (http://cccbdb.nist.gov/vibscalejust.asp) under the harmonic oscillator assumption. The numbers in square brackets represent the percent deviation of the predicted constant with respect to the fitted results with the corresponding experimental percentage uncertainty in parentheses. The calculated and predicted constants are for the equilibrium geometry.

Const. (cm^{-1})	Fit[a]	MP2(FULL)\6–31g(d)	CCSD\6-31+g(d)	B3LYP\6-31+g(d)
A''	0.73948 (9)	0.74070 [−0.165 (12)]	0.73767 [0.245 (12)]	0.74317 [−0.499 (12)]
B''	0.12807 (8)	0.12916 [−0.851 (62)]	0.12738 [0.539 (62)]	0.12649 [1.234 (62)]
C''	0.11920 (8)	0.11995 [−0.629 (67)]	0.11843 [0.646 (67)]	0.11776 [1.208 (67)]
$\tilde{\epsilon}''_{aa}=-(a_0+2a)''$	−0.0548 (17)	−0.0463 (15) [16. (63)]	−0.0460 (15) [16. (63)]	−0.0462 (15) [16. (3)]
$\tilde{\epsilon}''_{bb}=(a+b-a_0)''$	−0.0016 (15)	−0.0028 (14) [−75. (94)]	−0.0027 (14) [−69. (94)]	−0.0028 (14) [−75. (94)]
$\tilde{\epsilon}''_{cc}=(a-b-a_0)''$	−0.0003 (16)	−0.0001 (15) [67. (533)]	−0.0001 (15) [67. (533)]	−0.0001 (15) [67. (533)]
$(1/2)(\tilde{\epsilon}_{ab}+\tilde{\epsilon}_{ba})''=d''$	0.0009 (28)	0.0029 (22) [−222. (311)]	0.0030 (22) [−233. (311)]	0.0032 (22) [−256. (311)]
$(1/2)(\tilde{\epsilon}_{bc}+\tilde{\epsilon}_{cb})''=c''$	0	0	0	0
$(1/2)(\tilde{\epsilon}_{ac}+\tilde{\epsilon}_{ca})''=e''$	0	0	0	0
A'	0.72522 (9)	0.72511 [0.015 (12)]	0.72220 [0.416 (12)]	0.72977 [−0.627 (12)]
B'	0.12866 (8)	0.12953 [−0.676 (52)]	0.12747 [0.925 (62)]	0.12657 [1.624 (62)]
C'	0.11928 (8)	0.11987 [−0.537 (67)]	0.11813 [0.923 (67)]	0.11752 [1.434 (67)]
$\tilde{\epsilon}'_{aa}=-(a_0+2a)'$	0.0507 (19)	0.0496 (15) [2. (4)]	0.0492 (15) [3. (4)]	0.0488 (15) [4. (4)]
$\tilde{\epsilon}'_{bb}=(a+b-a_0)'$	0.0016 (15)	0.0029 (14) [−81. (94)]	0.0029 (14) [−81. (94)]	0.0030 (14) [−88. (94)]
$\tilde{\epsilon}'_{cc}=(a-b-a_0)'$	−0.0011 (16)	−0.0012 (15) [−9. (145)]	−0.0012 (15) [−9. (145)]	−0.0012 (15) [−9. (145)]
$(1/2)(\tilde{\epsilon}_{ab}+\tilde{\epsilon}_{ba})'=d'$	−0.0020 (98)	−0.0088 (22) [−340. (490)]	−0.0089 (22) [−345. (490)]	−0.0095 (22) [−375. (490)]
$(1/2)(\tilde{\epsilon}_{bc}+\tilde{\epsilon}_{cb})'=c'$	0	0	0	0
$(1/2)(\tilde{\epsilon}_{ac}+\tilde{\epsilon}_{ca})'=e'$	0	0	0	0
T_{00}	7354.6377 (12)	7351.4572 [0.04]	6916.2306 [5.96]	7501.4582 [2.00]

[a]Fit temperature of T=73.2 K. By symmetry only the c component of the dipole moment is nonzero.

ratus, since the T conformer would have negligible population if the conformers were in equilibrium at the 15 K rotational temperature typical of the apparatus.[26]

We were able to record the spectra of both the normal and deuterated species of the G conformer with a good signal to noise ratio (S/N≈60–100 for the strongest features). Figure 1, a scan over about 20 cm^{-1} of the two isotopologues, shows that the spectra are highly congested, primarily due to the population of many rotational and spin-rotational levels even at a temperature of ≈15 K. Because of this congestion, assignments of spectral features to individual transitions are mostly impossible.

Due to the inability to assign individual lines, use of the traditional LSF method to simulate the spectrum and obtain the best values of the molecular parameters is counterindicated. We therefore have employed the EA approach described in Sec. IV A to simulate the spectra and determine the molecular parameters contained in the $\mathcal{H}_T$ [Eq. (1)] for each the $\tilde{A}$ and $\tilde{X}$ states.

Because it is somewhat more resolved (see below for details) we first analyzed the spectrum of the $C_2D_5O_2$ G radical using the EA approach. The fitted constants are summarized in Table I. The converged result of the EA not only produces the best values for the fit constants but at the same time the quantum numbers of the individual transitions are assigned. This allows a classical least-squares fit using the assigned frequencies. In Meerts and Schmitt[39] this is called an "assigned fit," and the definitions of the statistical errors and correlation coefficients are discussed in Appendix B of that paper. The errors reported in Table I are based on a 0.01 cm^{-1} uncertainty in the experimental line positions.

Figure 2 shows portions of the resulting simulation and parameters. The best agreement between the experimental spectrum and the fit was obtained with a rotational temperature of 15 K and with a fixed Gaussian component of 250 (Ref. 27) and 450 MHz for the Lorentzian component of a Voigt profile for individual transitions.

Figure 2 shows the simulation and observed spectra are virtually indistinguishable, which clearly shows the ability of the EA approach to successfully fit the molecular parameters and simulate the spectrum. Furthermore Table I shows that all 15 molecular parameters involved in $\mathcal{H}_T$ for the $\tilde{A}$ and $\tilde{X}$ states are well determined. Indeed the rotational constants

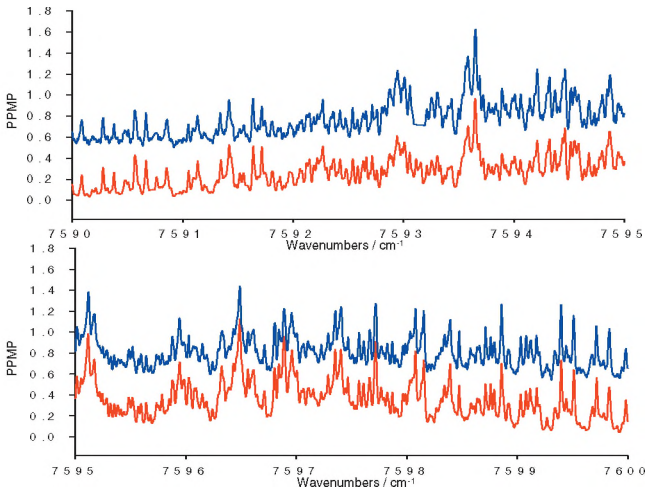

FIG. 2. Expanded scale for the $C_2D_5O_2$ radical G conformer. The top blue traces are the experimental spectrum shifted upward by 0.5 ppmp while the bottom red traces are the simulations based upon the fit constants in Table I. Axis conventions are the same as Fig. 1.

are determined to ≈10 ppm and the smaller spin-rotational constants, while having larger percentage errors, have similar absolute precision.

The components of the transition dipole along the principal axes given in Tables I and II are determined from the fit values of θ and ϕ using the relationships,

$$\mu_a = \mu \sin \phi \cos \theta, \tag{19}$$

$$\mu_b = \mu \sin \phi \sin \theta, \tag{20}$$

$$\mu_c = \mu \cos \phi. \tag{21}$$

Perhaps even more remarkable is that the experimental precision of the parameters for ethyl peroxy is very comparable to that which we previously reported for CD_3O_2, although in the former case individual transitions were mostly resolved and the parameters were determined from the transition frequencies by a LSF approach. While this result is counterintuitive, we expect that the high precision obtained in the present G $C_2D_5O_2$ spectrum fit is attributable to the fact that the EA approach uses both the (somewhat less precise) frequencies for the ethyl peroxy transitions *and* the intensity information contained in the $C_2D_5O_2$ spectrum while the LSF method used only the transition frequency information for CD_3O_2. Since CRDS is an absorption-based technique even absolute intensities are reliable, and the EA approach is ideal for fitting even highly congested CRDS spectra.

As with any fitting procedure, there is always a question as to whether the final parameters set (chromosome) is unique. One way of answering that question is to look at the fit molecular parameters and compare them to those resulting from quantum chemistry calculations. Since we expect all the quantum chemistry methods described in Sec. V to be relatively accurate, significant discrepancies between calculated and experimental results are neither expected nor are they found as is shown in Table I. Therefore we accept the fit parameters to be valid and in turn use them to judge the relative adequacy of the computational methods. It appears obvious that the MP2(FULL) method with a 6–31g(d) basis set reproduces quite well the experimental constants (within 0.3% for the rotational constants). The CCSD method also reproduces the experimental constants rather well but it does not do as good as a job as MP2(FULL), the geometry optimization step of the G2 compound method. (However it should be remembered that these comparisons are between the values of the rotational constants calculated at the equilibrium position and the experimental values averaged over the vibrationless level.) Finally, the DFT method provides rotational constants that are within ≈3% of the fitted constants.

Turning our attention to the components of the spin-rotation tensor, we can easily see from Table I that these constants are well determined and that they are in generally good agreement with the predictions, thereby validating the method of Sec. V. It appears evident that, as for the rotational constants, the MP2(FULL) calculation best predicts the spin-rotation constants while the B3LYP predictions deviate fairly significantly from the fitted results. The explanation of the difference in accuracy is actually fairly simple. To derive the components of the spin-rotation tensors for a given molecule one needs a good optimized geometry. The rotational constants are best predicted by the MP2(FULL) method compared to the DFT method implying the optimized geometry of this method is most accurate, so MP2(FULL) should also be best at predicting the spin-rotation parameters, which again depend upon this geometry.

As Table I shows we actually only used the real part of the spin-rotation tensor to fit our spectrum. This result is partially predicated upon practicality. The EA program has not been adapted to diagonalize a complex $\mathcal{H}_T$ matrix. However, this approximation was justified by using our SPECVIEW program[38] which can handle complex matrices. By adding the estimated values for c and e from the MP2(FULL) prediction into $\mathcal{H}_T$ and by examining the resulting predicted spectrum from SPECVIEW the largest shift in frequency is found to be ≈16.5 MHz, which, at our resolution, is not significant. This approximation is further confirmed by comparing SPECVIEW simulations including or not the two extra imaginary components of the spin-rotation tensor.

Table I also summarizes the calculated excitation energy T_{00} for all three electronic structure methods. The MP2(FULL) energy separation has been obtained by calculating both electronic states with the G2 compound method, which contains not only the ZPE correction but also several higher order energy correction terms. The CCSD and B3LYP energies are corrected by the ZPE correction under the harmonic oscillator approximation. It is no surprise that the MP2(FULL) energy calculation is the most accurate one as has been pointed out previously by Sharp *et al.*[20] On the other hand, it is more surprising that the CCSD calculation is less accurate than the B3LYP calculation since its global minimum structure of the radical appears to be more accurate that the B3LYP one. The explanation for this inadequacy could lie in the fact that the ZPE correction comes, obviously, from the calculation of the normal mode frequencies of the molecule and it is well known that the result of a frequency calculation using a CCSD method will be less accurate than the one coming from a B3LYP calculation.

Since the G conformer of the ethyl peroxy radical has C_1 symmetry, nonvanishing components of the transition dipole moment lie along all three axes, a, b and c. The calculated and experimental results are again summarized in Table I. Somewhat larger errors are present between experiment and calculations for the relative components of the transition dipole than for the $\tilde{A}$ and $\tilde{X}$ state parameters. However transition dipoles are notoriously difficult to calculate and likely the nearly forbidden nature of the $\tilde{A}-\tilde{X}$ transition makes it even a greater challenge. The fairly significant variation of the calculated dipoles using the three different optimized geometries, which are really quite similar, supports this supposition.

We have performed a similar analysis for the $C_2H_5O_2$ isotopologue. This experimental spectrum has been simulated at a rotational temperature of 16 K with a Voigt profile with a Gaussian component of 250 MHz and a Lorentzian component of 1400 MHz. A similar variation in the Lorent-

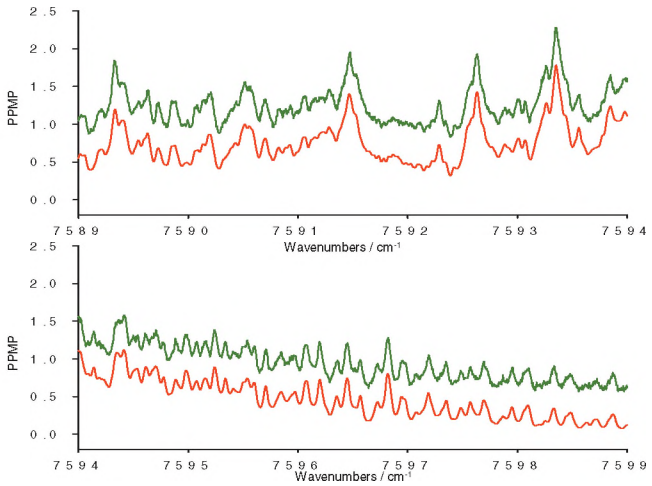

FIG. 3. Expanded scale for the $C_2H_5O_2$ radical G conformer. The top green traces are the experimental spectrum shifted upward by 0.5 ppmp while the bottom red traces are the fitted spectra using the constants in Table II. Axis conventions are the same as Fig. 1.

zian components for CD_3O_2 and CH_3O_2 was previously noted.[50] The most probable explanation is that the Lorentzian component results from lifetime broadening in the $\tilde{A}$ state perhaps due to internal conversion, which is more facile in the H isotopologue. At present, analyses are proceeding on the spectra of propyl and phenyl peroxy. When these are complete we hope to be able to publish a more complete explanation of this interesting phenomenon.

The results for $C_2H_5O_2$ are summarized in Table II and in Fig. 3. It is clear that the simulated spectra are again in near perfect agreement with the experimental trace. Comparing the experimental and calculated parameters in Table II we came to the same conclusion, i.e., MP2(FULL) makes the best predictions for molecular parameters while, of the three, the B3LYP method predicts most poorly. However, the agreement between the predicted and the fitted molecular parameters is poorer by a factor of ≈2 for $C_2H_5O_2$ compared to $C_2D_5O_2$. This can be explained by the fact that the $C_2H_5O_2$ spectrum is not as resolved as its isotopologue.

We have also obtained the spectra for the $C_2H_5O_2$ and $C_2D_5O_2$ radicals under somewhat warmer conditions obtained by reducing the backing pressure upstream of our slit jet. Figure 4 confirms the parameters from the 15 K spectra well simulate the warmer $C_2H_5O_2$ spectrum (fit at 32 K) and that of $C_2D_5O_2$ (fit at 28 K).

B. The T conformer of the ethyl peroxy radical

Since the T conformer of the ethyl peroxy radical has C_s symmetry, its electronic transition dipole moment lies along the c-axis and the spin-rotation tensor components c and e are equal to zero by symmetry. Normally, this would give the T conformer a simpler and somewhat stronger spectrum. However, Rupper *et al.*[17] calculated that in the ground electronic state, the T conformer lies about 80 cm^{-1} above the G conformer. Under equilibrium conditions at T≈15 K, we could expect the ratio of populations between the T and the G conformer would be of

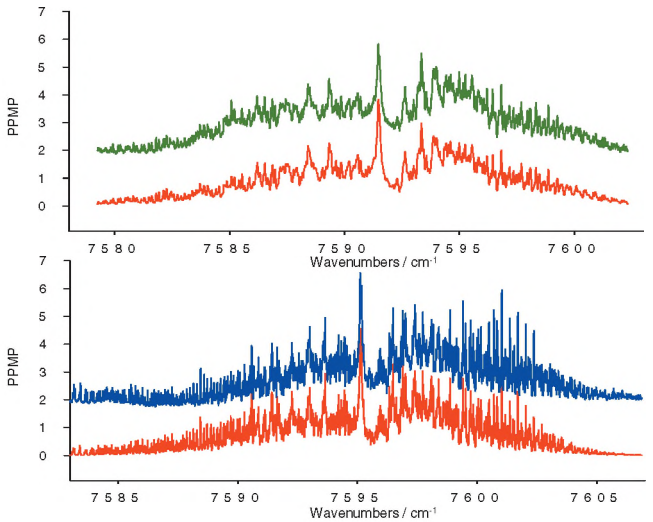

FIG. 4. Experimental and simulation of the warmer spectra of the normal and deuterated ethyl peroxy radical G conformer. The top panel represents the normal isotopologue with the top green trace the experimental spectrum and the bottom red trace the simulation using the fitted constants in Tables III and IV. The bottom panel represents the deuterated isotopologue with the experimental spectrum on top and its simulation at the bottom. For both sets of traces, the experimental spectrum has been shifted upward by 2.0 ppmp. Axis conventions are the same as Fig. 1.

$$\frac{N_T}{N_G} = \frac{1}{2}e^{-7.7} = 4.7 \times 10^{-4}, \tag{22}$$

where the factor of 1/2 results from the two mirror image enantiomers of the G conformer. Nonetheless, we decided to search for the T conformer, albeit at somewhat higher temperatures using lower backing pressures. We were able to record warmer spectra for both $C_2H_5O_2$ and $C_2D_5O_2$, which are shown with their simulations, in Figs. 5 and 6, respectively. The rotational temperatures were found to be 99 K for the normal species and 73 K for the deuterated one. Thereafter we also observed T conformer spectra under the 15 K

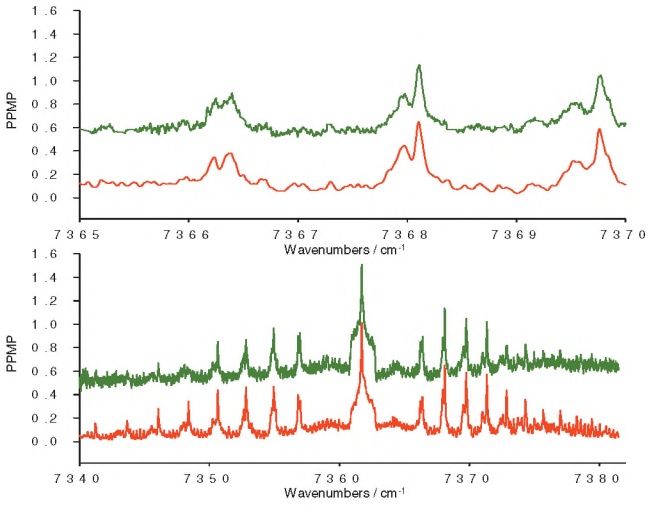

FIG. 5. Experimental and simulated spectra of the T conformer of the $C_2H_5O_2$ radical. The upper panel shows an enlargement of a 5 cm^{-1} section of the lower panel. In each panel, the top trace is the experimental spectrum shifted upward by 0.5 ppmp while the bottom trace is the simulated spectrum, using the fitted constants in Table III. Axis conventions are the same as Fig. 1.

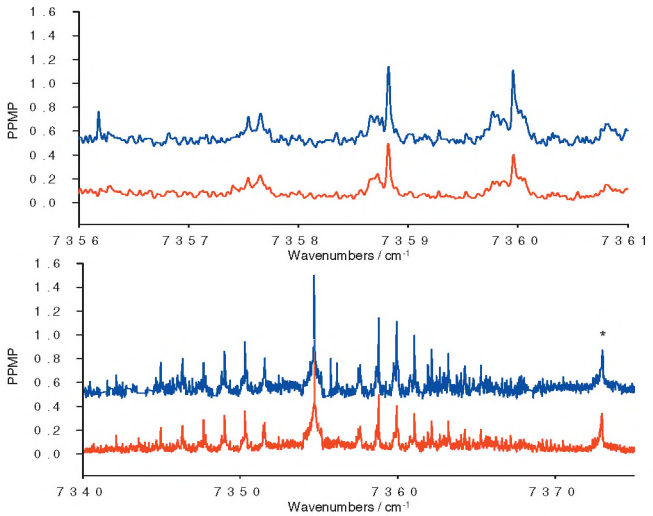

FIG. 6. Experimental and simulated spectra of the T conformer of the $C_2D_5O_2$ radical. The upper panel shows an enlargement of a 5 cm^{-1} section of the lower panel. In each panel, the top trace is the experimental spectrum shifted upward by 0.5 ppmp while the bottom trace is the simulated spectrum using the fitted constants in Table IV. The star represents the CD_3O_2 radical that was also observed in the experiment. The constants used to simulate it are the ones published by Wu *et al.* (Ref. 27).

rotational temperature conditions, although with relatively low signal/noise ($\lesssim$5). These observations allow us to reach the conclusion that, in our slit jet expansion, the conformers are not in thermal equilibrium with the rotations.

Looking carefully at Fig. 6, one can see on the blue end of the spectrum a broad feature, which was found and fitted to be the 0_0^0 band of the CD_3O_2 radical. The constants used to fit this unexpected band have been fixed to the ones published by Wu *et al.*[27] and only the rotational temperature was fitted in this simulation and was found to be 83 K. The individual line shapes employed in the simulations for the T conformer were similar to the ones used for the G conformer, i.e., Voigt profiles with a Gaussian component of 445 MHz due to the increased Doppler broadening at higher temperature and a Lorentzian component of 1400 MHz for the normal species and 450 MHz for the deuterated one.

Tables III and IV show the calculated and predicted rotational and spin-rotational constant for the normal and the deuterated isotopes of the T conformer of the ethyl peroxy radical. Looking at these results it appears for the $\tilde{X}$ state of the T conformer the CCSD method is equal or perhaps even better than the MP2(FULL) method. However, the DFT method still lags these two techniques and gives more qualitative predictions. When looking at the first excited state calculated and predicted constants, the same trend as for the G conformer can be found, i.e., the MP2(FULL) predictions are closer to the fitted values than the CCSD.

Finally, if one compares the errors between both isotopologues of the T conformer of the ethyl peroxy radical, one can see that they are almost equivalent, which is unexpected due to the fact that the Lorentzian component of the Voigt profile of the perdeutero is significantly smaller than the perproteo. This can be rationalized by the fact that a significantly larger water absorption is present in this part of the electromagnetic spectrum leading to poorer background subtraction, which explains the unexpectedly larger errors on the fitted molecular constants of the perdeutero species.

VII. CONCLUSION

We have successfully recorded the partially rotationally resolved spectra for both conformers (G and T) of the ethyl peroxy radical, $C_2H_5O_2$ and its perdeutero analog, $C_2D_5O_2$. We have used an EA approach to analyze the observed spectra. This approach has yielded simulated spectra virtually indistinguishable from the experimental traces and produced a set of molecular parameters characterizing the $\tilde{X}$ and $\tilde{A}$ states of the radicals.

In earlier room temperature work on ethyl peroxy it was recognized that the spectra of two conformers clearly existed. The assignment of the two origin bands to given conformers was initially based upon an *ab initio* prediction that the T conformer origin was at lower frequency. Support for this assignment was given by an analysis[17] of the rotational contours of the band. Obtaining a complete set of rotational constants characterizing the respective bands and comparing them to those expected based upon the conformers' geometries removes any remaining doubt about the conformer assignment.

Furthermore, comparison (see Tables I–IV) of the experimental parameters with those from electronic structure calculation allows us to benchmark the latter. We have further demonstrated that we were able to predict the observed spin-rotation constants using the isotopic substitution approach proposed by Brown, Sears, and Watson[37] and extended by Tarczay *et al.*[49]

The fact that we were able to obtain and analyze spectra from the higher energy T conformer leads to the conclusion that in our jet expansion, the conformers are not produced in thermal equilibrium. This work shows that observing *and* analyzing the spectra of even larger radicals are quite feasible.

ACKNOWLEDGMENTS

The authors gratefully acknowledge the support of the U.S. National Science Foundation via Grant No. CHE-0511809 and the Ohio Supercomputer Center.

[1] P. D. Lightfoot, R. A. Cox, J. N. Crowley, M. Destriau, G. D. Hayman, M. E. Jenkin, G. K. Moortgat, and F. Zabel, Atmos. Environ. **26A**, 1805 (1992).
[2] G. S. Tyndall, R. A. Cox, C. Granier, R. Lesclaux, G. K. Moortgat, M. J. Pilling, A. R. Ravishankara, and T. J. Wallington, J. Geophys. Res. **106**, 12157 (2001).
[3] M. J. Pilling, *Chemical Kinetics, Low-Temperature Combustion and Autoignition* (Elsevier, Amsterdam, 1997), Vol. 35.
[4] T. J. Wallington and O. J. Nielsen, *Peroxyl Radicals* (Wiley, New York, 1997), p. 457.
[5] G. J. Frost, G. B. Ellison, and V. Vaida, J. Phys. Chem. A **103**, 10169 (1999).
[6] H. J. Curran, P. Gaffuri, W. J. Pitz, and C. K. Westbrook, Combust. Flame **114**, 149 (1998).
[7] H.-H. Carstensen, C. V. Naik, and A. M. Dean, J. Phys. Chem. A **109**, 2264 (2005).
[8] T. A. Miller, Mol. Phys. **104**, 2581 (2006).
[9] T. J. Wallington, P. Dagaut, and M. J. Kurylo, Chem. Rev. **92**, 667 (1992).
[10] J. A. Jafri and D. H. Phillips, J. Am. Chem. Soc. **112**, 2586 (1990).

[11] O. J. Nielsen and T. J. Wallington, *Peroxyl Radicals* (Wiley, New York, 1997), p. 69.
[12] H. E. Hunziker and H. R. Wendt, J. Chem. Phys. **64**, 3488 (1976).
[13] M. B. Pushkarsky, S. J. Zalyubovsky, and T. A. Miller, J. Chem. Phys. **112**, 10695 (2000).
[14] S. J. Zalyubovsky, B. G. Glover, T. A. Miller, C. Hayes, J. K. Merle, and C. M. Hadad, J. Phys. Chem. A **109**, 1308 (2005).
[15] G. Tarczay, S. J. Zalyubovsky, and T. A. Miller, Chem. Phys. Lett. **406**, 81 (2005).
[16] B. G. Glover and T. A. Miller, J. Phys. Chem. A **109**, 11191 (2005).
[17] P. Rupper, E. N. Sharp, G. Tarczay, and T. A. Miller, J. Phys. Chem. A **111**, 832 (2007).
[18] C.-Y. Chung, C.-W. Cheng, Y.-P. Lee, H.-Y. Liao, E. N. Sharp, P. Rupper, and T. A. Miller, J. Chem. Phys. **127**, 044311 (2007).
[19] E. N. Sharp, P. Rupper, and T. A. Miller, J. Phys. Chem. A **112**, 1445 (2008).
[20] E. N. Sharp, P. Rupper, and T. A. Miller, Phys. Chem. Chem. Phys. **10**, 3955 (2008).
[21] S. J. Blanksby, T. M. Ramond, G. E. Davico, M. R. Nimlos, S. Kato, V. M. Bierbaum, W. C. Lineberger, G. B. Ellison, and M. Okumura, J. Am. Chem. Soc. **123**, 9585 (2001).
[22] G. Meloni, P. Zou, S. J. Klippenstein, M. Ahmed, S. R. Leoni, C. A. Taatjes, and D. L. Osborn, J. Am. Chem. Soc. **128**, 13559 (2006).
[23] D. B. Atkinson and J. L. Spillman, J. Phys. Chem. A **106**, 8891 (2002).
[24] H. B. Fu, Y. J. Hu, and E. R. Bernstein, J. Chem. Phys. **125**, 014310 (2006).
[25] P. Dupré and T. A. Miller, Rev. Sci. Instrum. **78**, 033102 (2007).
[26] S. Wu, P. Dupré, and T. A. Miller, Phys. Chem. Chem. Phys. **8**, 1682 (2006).
[27] S. Wu, P. Dupré, P. Rupper, and T. A. Miller, J. Chem. Phys. **127**, 224305 (2007).
[28] L. S. Rothman, D. Jacquemart, A. Barbe, D. C. Benner, M. Birk, L. R. Brown, M. R. Carleer, C. Chackerian, J. K. Chance, L. H. Coudert, V. Dana, V. M. Devi, J. M. Flaud, R. R. Gamache, A. Goldman, J. M. Hartmann, K. W. Jucks, A. G. Maki, J. Y. Mandin, S. T. Massie, J. Orphal, A. Perrin, C. P. Rinsland, M. A. H. Smith, J. Tennyson, R. N. Tolchenov, R. A. Toth, J. V. Auwera, P. Varanasi, and G. Wagner, J. Quant. Spectrosc. Radiat. Transf. **96**, 139 (2005).
[29] S. Gopalakrishnan, C. C. Carter, L. Zu, V. Stakhursky, G. Tarczay, and T. A. Miller, J. Chem. Phys. **118**, 4954 (2003).
[30] R. N. Zare, *Angular Momentum* (Wiley Interscience, New York, 1988).
[31] J. H. Van Vleck, Rev. Mod. Phys. **23**, 213 (1951).
[32] W. T. Raynes, J. Chem. Phys. **41**, 3020 (1964).
[33] R. F. Curl and J. L. Kinsey, J. Chem. Phys. **35**, 1758 (1961).
[34] A. Carrington and B. J. Howard, Mol. Phys. **18**, 225 (1970).
[35] X. Q. Tan, J. M. Williamson, S. C. Foster, and T. A. Miller, J. Phys. Chem. **97**, 9311 (1993).
[36] J. M. Brown and T. J. Sears, J. Mol. Spectrosc. **75**, 111 (1979).
[37] J. M. Brown, T. J. Sears, and J. K. G. Watson, Mol. Phys. **41**, 173 (1980).
[38] V. L. Stakhursky and T. A. Miller, 56th OSU International Symposium on Molecular Spectroscopy, The Ohio State University, Columbus, 2001, Vol. TC06, p. 107.
[39] W. L. Meerts and M. Schmitt, Int. Rev. Phys. Chem. **25**, 353 (2006).
[40] G. Myszkiewicz, W. L. Meerts, C. Ratzer, and M. Schmitt, J. Chem. Phys. **123**, 044304 (2005).
[41] J. A. Hageman, R. Wehrens, R. de Gelder, W. L. Meerts, and L. M. C. Buydens, J. Chem. Phys. **113**, 7955 (2000).
[42] W. L. Meerts, M. Schmitt, and G. Groenenboom, Can. J. Chem. **82**, 804 (2004).
[43] N. Hansen and A. Ostermeier, Evol. Comput. **9**, 159 (2001).
[44] A. Ostenmeier, A. Gawelcyk, and N. Hansen, *Parallel Problem Solving from Nature, PPSN III* (Springer, Berlin, 1994), Vol. 3.
[45] I. Kalkman, C. Vu, M. Schmitt, and W. L. Meerts, ChemPhysChem **9**, 1788 (2008).
[46] I. Kalkman, C. Brand, T.-B. C. Vu, W. L. Meerts, Y. N. Svartsov, O. Dopfer, K. Mueller-Dethlefs, S. Grimme, and M. Schmitt, J. Chem. Phys. **130**, 224303 (2009).
[47] M. J. Frisch, G. W. Trucks, H. B. Schlegel *et al.*, GAUSSIAN 03, Revision C.02, Gaussian, Inc., Wallingford, CT, 2004.
[48] J. B. Foresman and Æ. Frisch, *Exploring Chemistry with Electronic Structure Methods*, 2nd ed. (Gaussian, Inc., Pittsburgh, PA, 1996).
[49] G. Tarczay, S. Gopalakrishnan, and T. A. Miller, J. Mol. Spectrosc. **220**, 276 (2003).
[50] J. Liu, M.-W. Chen, D. Melnik, T. A. Miller, Y. Endo, and E. Hirota, J. Chem. Phys. **130**, 074303 (2009).